

DTIC FILE COPY

ARO 24600-1-EG

②

AD-A191 805

BURIED OBJECT DETECTION

Kenneth E. Gilbert

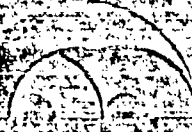
James M. Sabatier

DTIC
ELECTE
FEB 23 1988

3

D

CH



Institute for Technology Development

Turning ideas into innovations

DISTRIBUTION STATEMENT A

Approved for public release;
Distribution Unlimited

88 2 22 29 1

2

BURIED OBJECT DETECTION

Kenneth E. Gilbert

James M. Sabatier

Final Report

19 January 1987

Army Research Office

Contract No. DAAL03-87-K-0052

National Center for Physical Acoustics
P. O. Box 847
University, MS 38677

Approved for Public Release;
Distribution Unlimited.

S DTIC
ELECTE **D**
FEB 23 1988
H

SECURITY CLASSIFICATION OF THIS PAGE

REPORT DOCUMENTATION PAGE

1a. REPORT SECURITY CLASSIFICATION Unclassified		1b. RESTRICTIVE MARKINGS	
2a. SECURITY CLASSIFICATION AUTHORITY		3. DISTRIBUTION/AVAILABILITY OF REPORT Approved for public release; distribution unlimited.	
2b. DECLASSIFICATION/DOWNGRADING SCHEDULE		4. PERFORMING ORGANIZATION REPORT NUMBER(S)	
4. PERFORMING ORGANIZATION REPORT NUMBER(S)		5. MONITORING ORGANIZATION REPORT NUMBER(S) ARO 24600-1EG	
6a. NAME OF PERFORMING ORGANIZATION Institute for Technology Development	6b. OFFICE SYMBOL (if applicable)	7a. NAME OF MONITORING ORGANIZATION U. S. Army Research Office	
6c. ADDRESS (City, State, and ZIP Code) 700 North State Street; Suite 500 Jackson, MS 39202		7b. ADDRESS (City, State, and ZIP Code) P. O. Box 12211 Research Triangle Park, NC 27709-2211	
8a. NAME OF FUNDING/SPONSORING ORGANIZATION U. S. Army Research Office	8b. OFFICE SYMBOL (if applicable)	9. PROCUREMENT INSTRUMENT IDENTIFICATION NUMBER DAAO3-87-K-0052	
8c. ADDRESS (City, State, and ZIP Code) P. O. Box 12211 Research Triangle Park, NC 27709-2211		10. SOURCE OF FUNDING NUMBERS	
		PROGRAM ELEMENT NO.	PROJECT NO.
		TASK NO.	WORK UNIT ACCESSION NO.
11. TITLE (Include Security Classification) Buried Object Detection			
12. PERSONAL AUTHOR(S) James M. Sabatier and Kenneth E. Gilbert			
13a. TYPE OF REPORT Final	13b. TIME COVERED FROM 4/15/87 TO 4/14/88	14. DATE OF REPORT (Year, Month, Day) January 22, 1988	15. PAGE COUNT 18
16. SUPPLEMENTARY NOTATION The view, opinions and/or findings contained in this report are those of the author(s) and should not be construed as an official Department of the Army position, policy, or decision, unless so designated by other documentation.			
17. COSATI CODES		18. SUBJECT TERMS (Continue on reverse if necessary and identify by block number)	
FIELD	GROUP	Acoustic, Seismic, Acoustic seismic coupling, porefluid, pulse echo, propagation, soils, sound speed, attenuation, buried objects, detection	
19. ABSTRACT (Continue on reverse if necessary and identify by block number) When an airborne sound wave strikes the surface of the ground it reflects but also transmits as a pore-fluid wave and seismic body waves. The pore-fluid wave travels in the pores and through viscous drag as the pore walls transfer energy to the frame or soil matrix. As a consequence, this wave is highly attenuated and travels with a slow phase speed (100 dB/m, 10 m/s at 100 Hz) and is the source of seismic waves in the soil. Because the ground is weathered or layered (depths of tens of centimeters to meters) interferences between down and up going wave setup the steady-state interference minima and maxima that one observes in the seismic transfer function. An acoustic scheme for buried object detection is thought to involve a sound source above the ground and a microphone as a receiver. In the simplest scenario, an airborne acoustic pulse would be transmitted, strike the ground surface, propagate through the pores and reflect off the surface of a non-porous object. The microphone would then be used to detect the pore-fluid echo. These ideas were first considered in a sound tube with spherical beads.			
20. DISTRIBUTION/AVAILABILITY OF ABSTRACT <input type="checkbox"/> UNCLASSIFIED/UNLIMITED <input type="checkbox"/> SAME AS RPT. <input type="checkbox"/> DTIC USERS		21. ABSTRACT SECURITY CLASSIFICATION Unclassified	
22a. NAME OF RESPONSIBLE INDIVIDUAL		22b. TELEPHONE (include Area Code)	22c. OFFICE SYMBOL

UNCLASSIFIED

SECURITY CLASSIFICATION OF THIS PAGE

Used as the porous medium. Experimental measurements of the pore-fluid propagation constants were compared to rigid framed model calculations for model verification. These experimental and theoretical results were then used to make predictions of the sound levels required to detect objects buried a few centimeters in outdoor soils. In addition, we chose a detection criteria which required that the pore-fluid echo be at least $\frac{1}{2}$ cycle behind the pulse reflected from the ground surface. This criteria is quite arbitrary and conservative, but it allows for source specifications and from an experimental point of view appears as a realistic criteria for detection.

The models allowed for prediction of reflection losses, propagation losses, phase velocities and source levels based on burial depths of a few centimeters. Using these calculations various off-the-shelf acoustic sources were considered and it was realized that none were available to use existing sound sources to demonstrate that non-porous objects could be detected a few centimeters below the surface of institutional or grass soils. Research to develop a sound source which meets the original design criteria is on-going.

With modifications to off-the-shelf drivers, we were able to demonstrate that objects buried a few centimeters below the surface of a typical outdoor soil could be detected.

UNCLASSIFIED

SECURITY CLASSIFICATION OF THIS PAGE

BT
FOIA
b1
b7C
b7D
b7E
b7F
b7G
b7H
b7I
b7J
b7K
b7L
b7M
b7N
b7O
b7P
b7Q
b7R
b7S
b7T
b7U
b7V
b7W
b7X
b7Y
b7Z
b7AA
b7AB
b7AC
b7AD
b7AE
b7AF
b7AG
b7AH
b7AI
b7AJ
b7AK
b7AL
b7AM
b7AN
b7AO
b7AP
b7AQ
b7AR
b7AS
b7AT
b7AU
b7AV
b7AW
b7AX
b7AY
b7AZ
b7BA
b7BB
b7BC
b7BD
b7BE
b7BF
b7BG
b7BH
b7BI
b7BJ
b7BK
b7BL
b7BM
b7BN
b7BO
b7BP
b7BQ
b7BR
b7BS
b7BT
b7BU
b7BV
b7BW
b7BX
b7BY
b7BZ
b7CA
b7CB
b7CC
b7CD
b7CE
b7CF
b7CG
b7CH
b7CI
b7CJ
b7CK
b7CL
b7CM
b7CN
b7CO
b7CP
b7CQ
b7CR
b7CS
b7CT
b7CU
b7CV
b7CW
b7CX
b7CY
b7CZ
b7DA
b7DB
b7DC
b7DD
b7DE
b7DF
b7DG
b7DH
b7DI
b7DJ
b7DK
b7DL
b7DM
b7DN
b7DO
b7DP
b7DQ
b7DR
b7DS
b7DT
b7DU
b7DV
b7DW
b7DX
b7DY
b7DZ
b7EA
b7EB
b7EC
b7ED
b7EE
b7EF
b7EG
b7EH
b7EI
b7EJ
b7EK
b7EL
b7EM
b7EN
b7EO
b7EP
b7EQ
b7ER
b7ES
b7ET
b7EU
b7EV
b7EW
b7EX
b7EY
b7EZ
b7FA
b7FB
b7FC
b7FD
b7FE
b7FF
b7FG
b7FH
b7FI
b7FJ
b7FK
b7FL
b7FM
b7FN
b7FO
b7FP
b7FQ
b7FR
b7FS
b7FT
b7FU
b7FV
b7FW
b7FX
b7FY
b7FZ
b7GA
b7GB
b7GC
b7GD
b7GE
b7GF
b7GG
b7GH
b7GI
b7GJ
b7GK
b7GL
b7GM
b7GN
b7GO
b7GP
b7GQ
b7GR
b7GS
b7GT
b7GU
b7GV
b7GW
b7GX
b7GY
b7GZ
b7HA
b7HB
b7HC
b7HD
b7HE
b7HF
b7HG
b7HH
b7HI
b7HJ
b7HK
b7HL
b7HM
b7HN
b7HO
b7HP
b7HQ
b7HR
b7HS
b7HT
b7HU
b7HV
b7HW
b7HX
b7HY
b7HZ
b7IA
b7IB
b7IC
b7ID
b7IE
b7IF
b7IG
b7IH
b7II
b7IJ
b7IK
b7IL
b7IM
b7IN
b7IO
b7IP
b7IQ
b7IR
b7IS
b7IT
b7IU
b7IV
b7IW
b7IX
b7IY
b7IZ
b7JA
b7JB
b7JC
b7JD
b7JE
b7JF
b7JG
b7JH
b7JI
b7JJ
b7JK
b7JL
b7JM
b7JN
b7JO
b7JP
b7JQ
b7JR
b7JS
b7JT
b7JU
b7JV
b7JW
b7JX
b7JY
b7JZ
b7KA
b7KB
b7KC
b7KD
b7KE
b7KF
b7KG
b7KH
b7KI
b7KJ
b7KK
b7KL
b7KM
b7KN
b7KO
b7KP
b7KQ
b7KR
b7KS
b7KT
b7KU
b7KV
b7KW
b7KX
b7KY
b7KZ
b7LA
b7LB
b7LC
b7LD
b7LE
b7LF
b7LG
b7LH
b7LI
b7LJ
b7LK
b7LL
b7LM
b7LN
b7LO
b7LP
b7LQ
b7LR
b7LS
b7LT
b7LU
b7LV
b7LW
b7LX
b7LY
b7LZ
b7MA
b7MB
b7MC
b7MD
b7ME
b7MF
b7MG
b7MH
b7MI
b7MJ
b7MK
b7ML
b7MN
b7MO
b7MP
b7MQ
b7MR
b7MS
b7MT
b7MU
b7MV
b7MW
b7MX
b7MY
b7MZ
b7NA
b7NB
b7NC
b7ND
b7NE
b7NF
b7NG
b7NH
b7NI
b7NJ
b7NK
b7NL
b7NM
b7NN
b7NO
b7NP
b7NQ
b7NR
b7NS
b7NT
b7NU
b7NV
b7NW
b7NX
b7NY
b7NZ
b7OA
b7OB
b7OC
b7OD
b7OE
b7OF
b7OG
b7OH
b7OI
b7OJ
b7OK
b7OL
b7OM
b7ON
b7OO
b7OP
b7OQ
b7OR
b7OS
b7OT
b7OU
b7OV
b7OW
b7OX
b7OY
b7OZ
b7PA
b7PB
b7PC
b7PD
b7PE
b7PF
b7PG
b7PH
b7PI
b7PJ
b7PK
b7PL
b7PM
b7PN
b7PO
b7PP
b7PQ
b7PR
b7PS
b7PT
b7PU
b7PV
b7PW
b7PX
b7PY
b7PZ
b7QA
b7QB
b7QC
b7QD
b7QE
b7QF
b7QG
b7QH
b7QI
b7QJ
b7QK
b7QL
b7QM
b7QN
b7QO
b7QP
b7QQ
b7QR
b7QS
b7QT
b7QU
b7QV
b7QW
b7QX
b7QY
b7QZ
b7RA
b7RB
b7RC
b7RD
b7RE
b7RF
b7RG
b7RH
b7RI
b7RJ
b7RK
b7RL
b7RM
b7RN
b7RO
b7RP
b7RQ
b7RR
b7RS
b7RT
b7RU
b7RV
b7RW
b7RX
b7RY
b7RZ
b7SA
b7SB
b7SC
b7SD
b7SE
b7SF
b7SG
b7SH
b7SI
b7SJ
b7SK
b7SL
b7SM
b7SN
b7SO
b7SP
b7SQ
b7SR
b7SS
b7ST
b7SU
b7SV
b7SW
b7SX
b7SY
b7SZ
b7TA
b7TB
b7TC
b7TD
b7TE
b7TF
b7TG
b7TH
b7TI
b7TJ
b7TK
b7TL
b7TM
b7TN
b7TO
b7TP
b7TQ
b7TR
b7TS
b7TT
b7TU
b7TV
b7TW
b7TX
b7TY
b7TZ
b7UA
b7UB
b7UC
b7UD
b7UE
b7UF
b7UG
b7UH
b7UI
b7UJ
b7UK
b7UL
b7UM
b7UN
b7UO
b7UP
b7UQ
b7UR
b7US
b7UT
b7UU
b7UV
b7UW
b7UX
b7UY
b7UZ
b7VA
b7VB
b7VC
b7VD
b7VE
b7VF
b7VG
b7VH
b7VI
b7VJ
b7VK
b7VL
b7VM
b7VN
b7VO
b7VP
b7VQ
b7VR
b7VS
b7VT
b7VU
b7VV
b7VW
b7VX
b7VY
b7VZ
b7WA
b7WB
b7WC
b7WD
b7WE
b7WF
b7WG
b7WH
b7WI
b7WJ
b7WK
b7WL
b7WM
b7WN
b7WO
b7WP
b7WQ
b7WR
b7WS
b7WT
b7WU
b7WV
b7WW
b7WX
b7WY
b7WZ
b7XA
b7XB
b7XC
b7XD
b7XE
b7XF
b7XG
b7XH
b7XI
b7XJ
b7XK
b7XL
b7XM
b7XN
b7XO
b7XP
b7XQ
b7XR
b7XS
b7XT
b7XU
b7XV
b7XW
b7XX
b7XY
b7XZ
b7YA
b7YB
b7YC
b7YD
b7YE
b7YF
b7YG
b7YH
b7YI
b7YJ
b7YK
b7YL
b7YM
b7YN
b7YO
b7YP
b7YQ
b7YR
b7YS
b7YT
b7YU
b7YV
b7YW
b7YX
b7YY
b7YZ
b7ZA
b7ZB
b7ZC
b7ZD
b7ZE
b7ZF
b7ZG
b7ZH
b7ZI
b7ZJ
b7ZK
b7ZL
b7ZM
b7ZN
b7ZO
b7ZP
b7ZQ
b7ZR
b7ZS
b7ZT
b7ZU
b7ZV
b7ZW
b7ZX
b7ZY
b7ZZ

THE VIEW, OPINIONS, AND/OR FINDINGS CONTAINED IN THIS REPORT ARE THOSE OF THE AUTHOR(S) AND SHOULD NOT BE CONSTRUED AS AN OFFICIAL DEPARTMENT OF THE ARMY POSITION, POLICY, OR DECISION, UNLESS SO DESIGNATED BY OTHER DOCUMENTATION.



Accession For	
NTIS GRA&I	<input checked="" type="checkbox"/>
DTIC TAB	<input type="checkbox"/>
Unannounced	<input type="checkbox"/>
Justification	
By _____	
Distribution/	
Availability Codes	
Dist	Avail and/or Special
A-1	

BURIED OBJECT DETECTION

TABLE OF CONTENTS

	Page
1.0 INTRODUCTION.....	1
2.0 PREVIOUS EXPERIMENTAL MEASUREMENTS	2
2.1 Experimental Apparatus.....	2
2.2 Pore-fluid Wave Propagation Constants	3
3.0 EXTENSION TO OUTDOOR SOILS.....	6
3.1 The Acoustic Source.....	7
3.2 Echoes From Outdoor Soils.	8
4.0 CONCLUSION AND RECOMMENDATION	12

Forward

The experimental work described in this report was performed by Dr. James M. Sabatier. The effort was administered and reviewed by Dr. Kenneth E. Gilbert. Questions concerning the technical content of the report should be addressed to Dr. Sabatier. Administrative questions should be directed to Dr. Gilbert.

BURIED OBJECT DETECTION

1.0 INTRODUCTION

Research at the University of Mississippi (UM) and the Institute for Technology Development (ITD) in the area of acoustic-to-seismic (A/S) coupling has been on going for several years.¹ The initial A/S coupling work was carried out between UM and the United States Army Waterways Experiment Station (WES).^{2,3} More recently, through the support of the Army Research Office, models have been developed^{4,5,6,7} which have been used to explain this interaction of sound with the ground. WES has continued to support a research effort in A/S coupling at UM and for over the past years we have come to understand the interaction of sound with the ground.

When an airborne sound wave strikes the surface of the ground it reflects but also transmits as a pore-fluid wave and seismic body waves. The pore-fluid wave travels in the pores and through viscous drag as the pore walls transfer energy to the frame or soil matrix. As a consequence, this wave is highly attenuated and travels with a slow phase spaced (100 dB/m, 10m/s at 100Hz) and is the source of seismic waves in the soil. Because the ground is weathered or layered (depths of tens of centimeters to meters) interferences between down and up going waves setup the steady-state interference minima and maxima that one observes in the seismic transfer function.^{6,7}

The research effort in buried object detection came about because of continued association with WES. Models which had been developed to understand and make predictions concerning A/S coupling were also used to make predictions concerning the detection of buried objects. As a consequence, we developed a three-phase effort related to buried object detection: surface seismic measurements using geophones, remote seismic measurements using a laser velocimeter and pore-fluid echoes. The latter of these three is the subject of this report. On going work in the other two areas has progressed rapidly and the success has led to a security review of the program.

An acoustic scheme for buried object detection is thought to involve a sound source above the ground and a microphone as a receiver. In the simplest scenario, an airborne acoustic pulse would be transmitted, strike the ground surface, propagate through the pores and reflect off the surface of a non-porous object. The microphone would then be used to detect the pore-fluid echo. These ideas were first considered in a sound tube with spherical beads used as the porous medium. Experimental measurements of the pore-fluid propagation constants were compared to rigid framed model calculations for model verification. These experimental and theoretical results were then used to make predictions of the sound levels required to detect objects buried a few centimeters in outdoor soils. In addition, we chose a detection criteria which required that the pore-fluid echo be at least 1/2 cycle behind the pulse reflected from the ground surface. This criteria is quite arbitrary and conservative, but it allows for source specifications and from an experimental point of view appears as a realistic criteria for detection.

The models allowed for prediction of reflection losses, propagation losses, phase velocities and source levels based on burial depths of a few centimeters. Using these calculations various off-the-shelf acoustic sources were considered and it was realized that none were available which met the design criteria without some relaxation. In this research effort, it was possible to use existing sound sources to demonstrate that non-porous objects could be detected a few centimeters below the surface of institutional or grass soils. Research to develop a sound source which meets the original design criteria is on-going.

2.0 PREVIOUS EXPERIMENTAL MEASUREMENTS OF THE PORE-FLUID WAVE

Measurements of the A/S coupling phenomena led us to use microphones which were designed to be buried below the surface of the ground. Using these microphones, it is possible to measure the pore-fluid wave propagation constants in outdoor soils. These measurements were critical to the understanding of how sound interacts within the ground and have explained the commonly assumed local reaction property of the ground.⁵

A question we were led to ask ourselves was, "Is it possible to observe a pore-fluid wave echo from the soil, and could it be used as an acoustic probe in soils"? It was decided to conduct scale model experiments in which the various physical properties of the porous media could be controlled in an attempt to make predictions of the feasibility of the pore-fluid probe idea.

In this section, the experimental apparatus and measured propagation constants in low resistivity stacks of porous glass beads are presented.

2.1 Experimental Apparatus

The experimental apparatus consisted of a large aluminum sound tube, solid dielectric transducer, pulse-echo circuit and the transmitting and receiving electronics. Acoustic measurements in sound tubes with transducers of this type have been conducted in this lab for many years.⁸ The tube used in these measurements was 7m x 0.25m in diameter and air-filled unconsolidated stacks of glass beads were used as the porous media in the tube which was positioned vertically. Figure 1 shows the sound tube, transducer, and how glass beads samples could be loaded into the tube for analysis.

At the upper end of the tube a 0.25m diameter solid dielectric transducer was positioned. This type dielectric transducer has also been used for many years⁸ and the main advantage in this work is it is a good plane wave source in the sound tube even at frequencies above cutoff in the tube. A fast analog switch (2MHz) was used to switch from the transit to receive mode. In addition, it is possible to design these transducers with high frequency response (1MHz) and modifications can be made to the back plates to increase the output

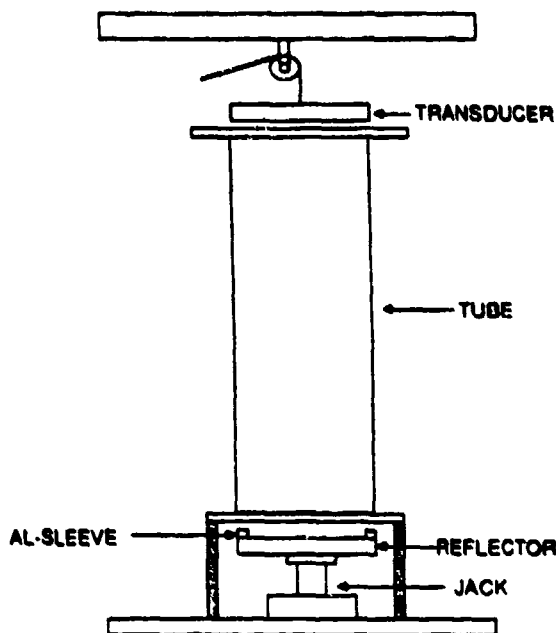


Figure 1. Sound tube configuration used in experimental work.

(at the expense of frequency response). This makes this transducer type suitable for the short tone burst used.

Typically, a two to four cycle tone burst with a peak voltage of 100 volts (rms) is delivered to the transducer. The acoustic return from the bottom of the tube (a few millivolts) is amplified and then displayed using a digital oscilloscope. Data can be sent to a mini-computer for storage and analysis via RS-232 interface between the computer and digital scope.

2.2 Pore-fluid Wave Propagation Constants

Initially, physical properties influencing propagation in stacks of spherical beads were determined. The beads used have bead diameters which range from 10mm to 1mm. Manufacturers of the beads indicate that these are less than 15% irregularly shaped particles and the sizes are as specified to within $\pm 0.2\text{mm}$. The beads were also smoothed and polished.

Measurements of the flow resistivity of the beads were made with a Leonards apparatus and the results are indicated in Table 1. In addition, the porosity was determined by

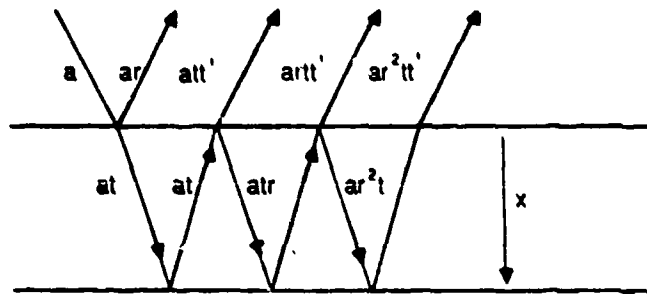
Spherical Glass Beads and Lead Shot

Size(mm)	Flow resistivity(rayls/cm)	Porosity
1.0	19.8 ± 2.0	.39
2.0	6.2 ± 0.70	.39
3.0	3.30 ± 0.34	.39
5.0	1.10 ± 0.12	.39
9.4 (lead)	(0.32) Calculated	.38

Table 1

measuring the volume of water necessary to fill the voids in a 100 cm^3 sample of beads. Measured values of the porosities of different beads sizes are shown in Table 1.

When an acoustic pulse is incident at the surface of the beads, it reflects from the surface but also bounces back and forth within the hard backed layer of beads producing an echo for each round trip it makes within the layer. Figure 2 schematically shows the phenomena.



Ray diagram of reflections from the surfaces of hardbacked layer of beads.

Figure 2

In Figure 2 the amplitude of the incident wave is a , the surface reflection coefficient is r , air-to-beads the transmission coefficient is t , the bead-to-air transmission coefficient is t' and the layer thickness is x . The first return has a magnitude

$$P_0 = ar. \tag{1}$$

The second return can be expressed as

$$P_1 = att'e^{-2\alpha x/20}, \quad (2)$$

Where α is the attenuation coefficient in dB per unit length. The logarithmic ratio of equations 1 and 2 is

$$\log\left(\frac{P_1}{P_0}\right) = \log\left(\frac{tt'}{r}\right) - 2\alpha x/20.$$

When the amplitudes of the first two echoes are plotted on a semilog scale as a function of layer thickness, the slope of the straight line is the attenuation coefficient in dB per unit length.

The pore-fluid wave phase speed was determined by measuring the time between the surface return and the first round trip return from within the stack of beads. Measured values from phase speed and attenuation coefficient are shown in Figures 3 and 4.

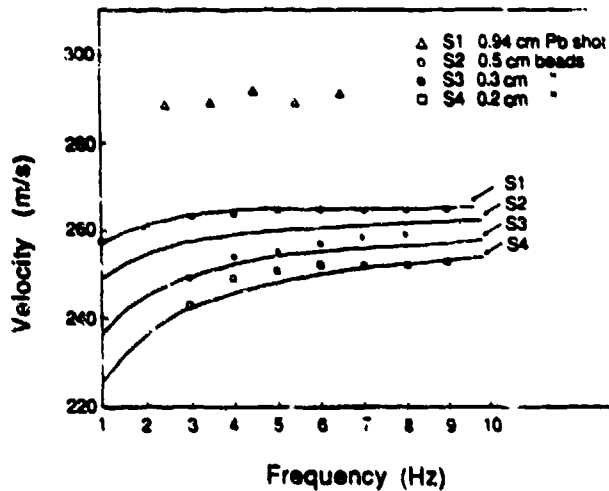


Figure 3

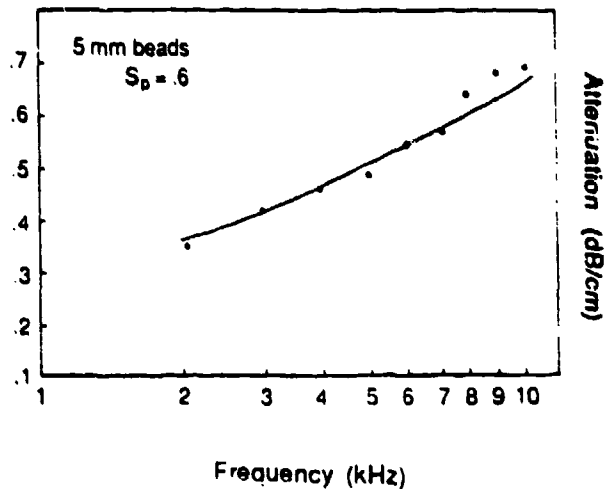


Figure 4

In the same figures are shown the theoretical values of the phase speed and attenuation constant. The calculations were made using the porous rigid frame model⁹ using the measured values of flow resistivity and porosity. The grain shape factor and pore shape factor ratio were typically 0.5 and 0.8, respectively. It can be observed that as the flow resistivity increased there is a trend for the experimental and theoretical calculation to agree.

3.0 EXTENSION TO OUTDOOR SOILS

The work described thus far indicates that it is possible to observe the pore fluid pulse in stacks of low resistivity glass beads. In order to observe this pulse in a realistic soil with a flow resistivity of 100-300cgs rayls/cm, the losses upon reflection at the ground surface and the pore-fluid attenuation must be considered. Realistic output levels of acoustic transducers, the penetration depth required and the soil reflection coefficient will determine the optimum frequency for the outdoor measurement.

A useful property of the rigid frame model is that it can be used to make predictions of both the reflection and propagation losses in soils. For frequencies above 2kHz, calculations indicate that the reflection losses when the pore-fluid transmits across the air-soil boundary twice will be less than 6 dB. Model calculations for this attenuation in a soil with a porosity of 0.269, and shape ratio of 0.28 and a flow resistivity of 300 rayls/cm are shown in Table 2.

Signal Loss

300 rayls/cm, $S_p = 0.28$, $\Omega = 0.269$, $n' = 0.5$

<u>min. frequency (Hz)</u>	<u>attenuation (dB/cm)</u>	<u>reflection losses (dB)</u>
100	.7	16.0
200	1.0	13.9
500	1.5	9.0
1 k	1.8	7.0
2 k	2.2	6.1
5 k	3.0	5.8
10 k	4.0	5.6
20 k	5.3	5.5
50 k	8.1	5.4
100 k	11.3	5.4

Table 2

There has been much experimental and theoretical work done related to pore-fluid properties in outdoor soils. The inputs used in the calculations shown in Table 2 are quite typical for soils and sands.

3.1 The Acoustic Source

Acoustic sources which meet the output levels indicated in Table 2 are available; however, there are other criteria to consider. The acoustic source must "turn off" such that the echo from the buried object can be observed behind the ground surface reflection. Since one or two cycles of a tone burst are used, the band width of the transducer must be sufficiently high to insure the high frequency Fourier components required to "turn off" the transducer are present. Because of the signal losses resulting from the ground properties and the expected time delay for the pore-fluid echo for a 10 kHz tone burst, a source with an output that is down 40 dB one cycle after turn-off time is desirable in order to observe the pore-fluid echo from a few centimeters below the soil surface.

Several off the shelf acoustic sources were considered; a 20kHz compression driver and horn, a 40 kHz leaf tweeter and a 30 kHz dome tweeter. In these transducers the turn off time is controlled by the upper frequency response. Consequently, the output wave form from these transducers was somewhat dissatisfactory. In addition to these three transducers the solid dielectric transducer was considered as a source. No single device of this type is capable of producing the required sound pressure levels.

Recent work at this lab,¹⁰ has shown that the frequency response of dielectric transducers can be precisely controlled. The frequency response of the solid dielectric transducer can be altered by changing the thickness of mylar, area of the backplate, tension on the diaphragm, and the roughness of the backing plate. The roughness of the backplate can be controlled by taking a smooth backplate which is only microscopically rough and applying an abrasive material, such as sandpaper or sand from sandblasting, to the surface. The result of this roughening is the replacement of most of the random microscopic cavities of roughly the same dimensions which have roughly the same resonant frequency. This results in a very narrow range of resonant frequencies with an increased sensitivity. The replacement of the majority of the smaller cavities with the larger cavities also results in the loss of high frequency response of transducer.

This same effect can be achieved by placing concentric grooves in the backplate which divides the backplate into two regions. The first region is the groove where the diaphragm is stretched over a cylindrical ringed cavity of trapped air. This region is similar to a standard capacitor microphone. The second region is the rail where the diaphragm is stretched over a cylindrical ringed backplate with air trapped in microscopic cavities. This is similar to a typical solid dielectric transducer. The total response of a transducer of this type is assumed to be the sum of the two regions. An array of dielectric transducers can be used to increase the output signal level. In current work, several such transducers are being used to achieve this goal and determine if the required pulse length can still be maintained.

Of the other three sources neither are capable of meeting the design criteria without further signal processing and design modifications. It was possible to make modifications to the 20 kHz compression driver that allowed it to be used in the outdoor experimental apparatus. The signal level was 40dB down 2 cycles after turn off as opposed to the design criteria of one cycle. Figure 5 is a diagram of the experimental apparatus with the acoustic

source. The horn driver was flush mounted to a 1m diameter piece of plexiglass. In addition the back of the driver was removed. Each of these steps had the effect of decreasing the effective period of the output pulse received by a 70kHz, 1/4 inch B and K microphone mounted between the driver and the ground. The modifications served to suppress the arrival of the horn's back wave and waves diffracted from the baffles outer rim so that the pore-fluid wave could be observed.

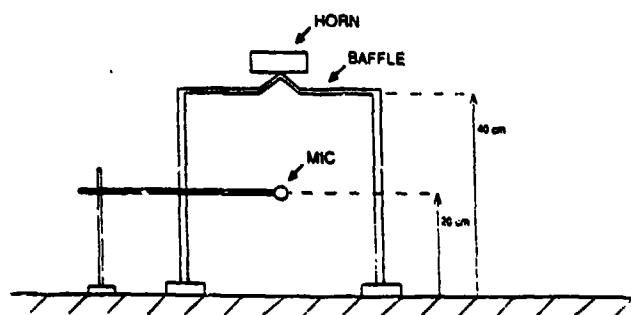


Figure 5. Experimental Apparatus

3.2 Echoes From Outdoor Soils.

The apparatus shown in Figure 5 was set up over a 80-100 square foot area of well spaded soil which had a measured flow resistivity of 40 c.g.s. rays/cm and moisture content of 20%. When the horn driver was pulsed for one cycle at 10 kHz, the first pulse received by the output was similar to that shown in Figure 6. The time traces of the microphone output were shifted so that the pulse leaving the horn or the incident pulse was at the far left side of the oscilloscope trace. A much higher band width source would improve the incident pulse shape as indicated in a previous section of this report.

Figures 6, 7, and 8 show the results of an experiment conducted over the spaded soil area. In Figure 6 the arrow indicates the time at which the echo from the soil surface is expected at the microphone. When a piece of plywood was placed directly over the soil, the amplitude of this echo was approximately the same size and had the same shape as the incident pulse. Figures 7 and 8 show the echo from the ground when a 33 cm diameter hollow metal cylinder, 10 cm in length was buried 1 cm and 5 cm below the soil surface, respectively. Two observations can be made. The amplitude of the echo is increased when the object is present, and the pulse shape and length are changed for each of the burial depths. It can be noted that the ground echoes are arriving earlier in time and this is because the top surface of the buried object was placed flush with the soil surface and then soil added to achieve the desired burial depth. When the non-porous hard object is buried below the surface, the ground surface impedance is increased and consequently the reflection coefficient

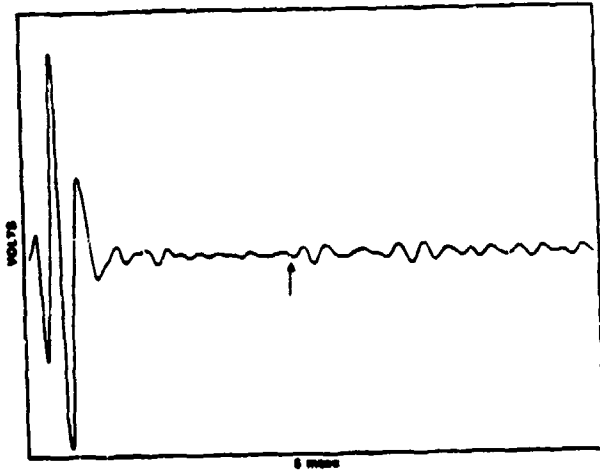


Figure 6

Echoes received from a large area of 40 rayl/cm soil.

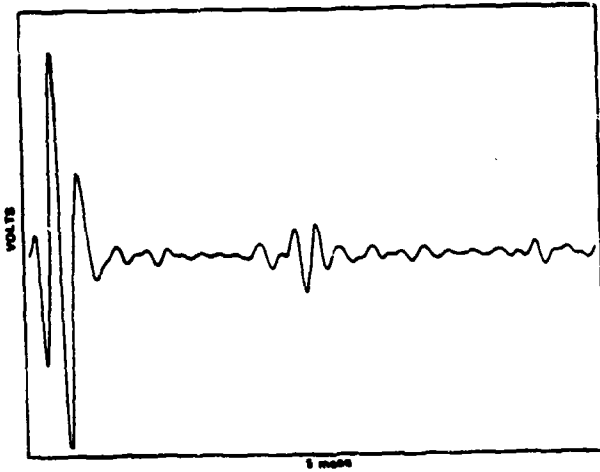


Figure 7

Echoes received from 40 rayl/cm soil when metal object was buried 1 cm below surface.

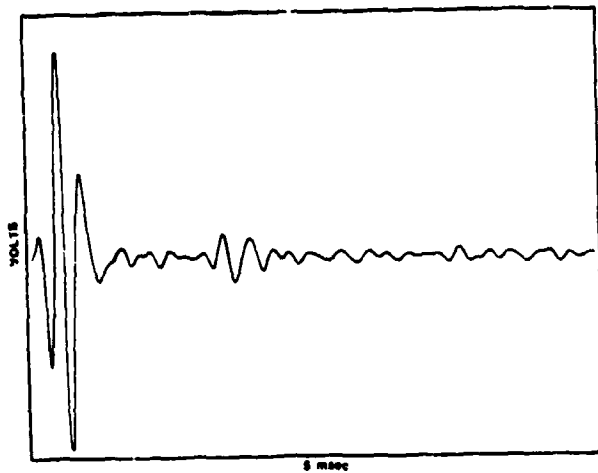


Figure 8

Echoes received from 40 rayl/cm soil when metal object was buried 5 cm below surface.

is increased resulting in a larger return. For this rather loose low flow resistivity soil, the amplitude change is sufficient for location of the buried object. There is not a separation between the surface and pore fluid echo but rather a smearing together. This results from the lack of homogeneity of the soil, the dispersive characteristic of the pore-fluid wave and the poor quality of the incident pulse.

In Figures 9, 10, and 11, the results of a somewhat different measurement are shown. The experimental apparatus was set up over an area of undisturbed grass or institutional soil as opposed to the large area of loose soil. The echo from the grass surface is shown in Figure 9. An additional echo (to those already described) at the far right of the time trace results from the reflection of the ground return at the horn baffle. In the previous site, the flow resistivity was 40 rayl/cm as opposed to 300 rayl/cm for this second site.

Next a 33 cm diameter, 15 cm deep cylindrical hole was dug and back-filled with the 40 rayls/cm loose soil. The resulting echo from this empty hole configuration is shown in Figure 10. This echo is observed to be smaller in amplitude than for undisturbed soil and 6-7 cycles long. Also note that the amplitude of the reflected pulse is larger than in previous measurement. This results because the reflected pulse reflects from an area larger than the 33cm diameter disturbed area. Good separation between the echo from the top of the soil-grass surface and the echo from the bottom of the 15cm deep hole is not achieved and consequently these echoes result in an extended pulse. Finally, the metal cylinder was placed in the hole with 3 cm of soil covering it. The echo observed is indicative of a less deep hole (see Figure 11). This echo does not "ring" for 6-7 cycles but rather 3 or 4. The superposition of the two echoes occurs in a shorter time period because the hole depth is less due to the presence of the hard object at 3 cm. The amplitude of the echoes in Figures 9, 10, and 11 are also different. The largest is for the undisturbed soil, and the smallest for the hole without the object. Disturbing the soil results in a decreased surface impedance (the flow resistivity goes from 300 rayls/cm to 40 rayls/cm) so that increased penetration (larger amplitude behind the incident pulse) is observed in Figures 10 and 11. In Figure 11 the propagation distance to the bottom of the hole is decreased because of the presence of the object and consequently the echo closely follows (in time) the incident pulse. Instead of the pulse traveling 30 cm in the soil, it propagated through only 10 cm of soil. In addition to that, the pore-fluid pulse is reflected from a non-porous hard surface which in this case results in reduced attenuation. Here, as in the previous measurement, the amplitudes of the ground returns are explained in terms of the effective surface impedance of the boundary. Also as before, the separation in surface and pore-fluid echo is not achieved.

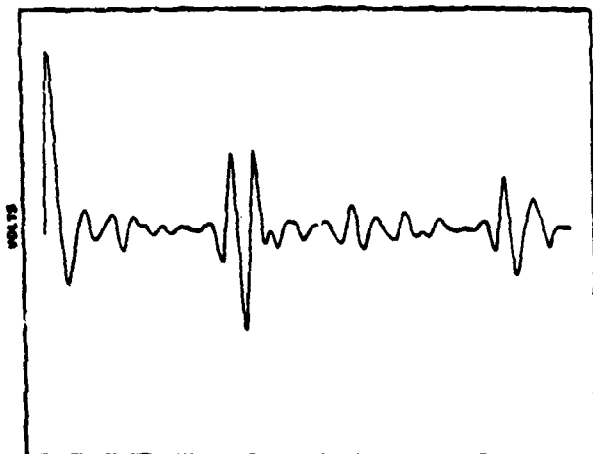


Figure 9

Echoes received from undisturbed 300 rayl/cm soil.

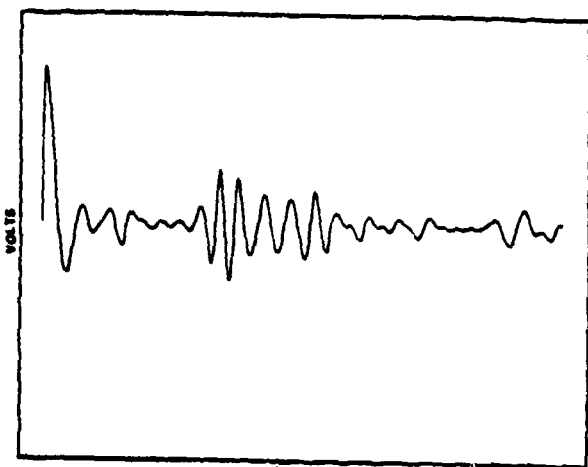


Figure 10

Echoes received from a hole formed in the soil.

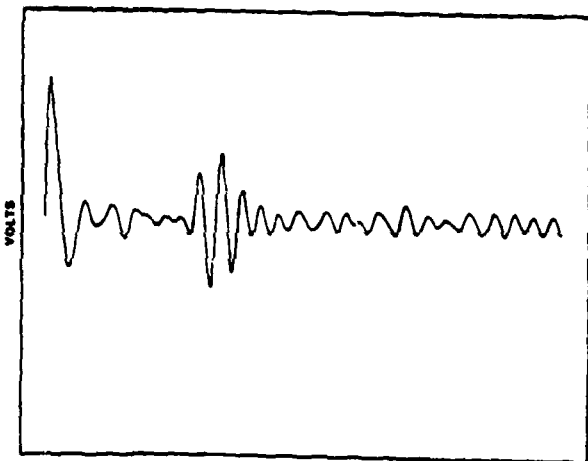


Figure 11

Echoes received when metal object was buried in the soil.

4.0 CONCLUSION AND RECOMMENDATION

In homogenous samples of glass beads it is possible to make measurements of pore-fluid echoes. These measurements yield values of the propagation constants that are explained in terms of the viscous effects at the pore walls and the rigid frame model calculations. The measurements were made in samples with flow resistivities much lower than for soils but model predictions indicate similar measurements can be made on outdoor soils. Indeed, continuous wave measurements of the pore fluid propagation constants in sandy soils have been done and model agreement was reasonable.⁵

Our initial calculations indicated that we would be able to observe the pore-fluid echo or separate the pore-fluid echo from the ground surface return. Because the source could not meet the design criteria, this observation was not made. But, we quickly learned that the amplitudes of the combined returns were significantly different to allow for buried object detection.

The results of the outdoor pulsed measurements to detect buried objects can be summarized as

1. The acoustic source used in the measurements did not allow for separation of the pore fluid echo from the surface echo for burial depths of 1-5 cm in the soils considered (and there are no better commercially available sources).
2. The dispersive characteristics of the pore fluid and the lack of homogeneity of the soil tend to smear the pore fluid echo and the surface return.
3. Even through the echo from the object cannot be cleanly separated from the surface return, the combined amplitude of the surface and pore fluid return's can nevertheless indicate the presence of objects buried 1-5cm below the soil.

The work done with the acoustic technique of buried object detection is promising and should continue. At this time we would recommend that work continue in two areas. First, the development of the acoustic source described in the designed criteria. Secondly, the work thus far has been driven by the detection in time domain of the pore fluid echo; a frequency analysis of the surface and pore fluid returns would allow for the interference phenomena associated with boundaries to be used in a detection scheme.

References

- 1 James M. Sabatier and K. E. Gilbert. "Method and Apparatus for Detecting Buried Objects by Measuring Seismic Vibrations Induced by Acoustical Coupling with a Remote Source of Sound"
- 2 M.D. Flohr and D.H. Cress, "Acoustic-to-Seismic Coupling: Properties and Applications to Seismic Sensors", Waterways Experiment Station Technical Rep. EL-79-1 (1979).
- 3 H.E. Bass, L.N. Bolen, Daniel Cress, Jerry Lundien, and Mark Flohr, "Coupling of Airborne Sound into the Earth: Frequency Dependence", J. Acoust. Soc. Am. 67, 1502-1506 (1980).
- 4 James M. Sabatier, Henry E. Bass, Lee N. Bolen and Keith Attenborough, "Acoustically Induced Seismic Waves," J. Acoust. Soc. Am. 80, 646-649 (1986).
- 5 James M. Sabatier, Henry E. Bass, Lee N. Bolen, Keith Attenborough, and V.V.S.S. Sastry, "The Interaction of Airborne sound with The Porous Ground: Theoretical Formulation," J. Acoust. Soc. Am. 79, 1345-1352 (1986).
- 6 James M. Sabatier, Henry E. Bass, Lee N. Bolen, and Keith Attenborough, "The Acoustic Transfer Function at the Surface of a Layered Poroelastic Soil," J. Acoust. Soc. Am. 79, 1353-1358 (1986).
- 7 James M. Sabatier, Henry E. Bass, and Glenn Elliott, "On the location of the frequencies of maximum acoustic-to-seismic coupling," J. Acoust. Soc. am. 80, 1200-1202 (1986).
- 8 F. Douglas Shields, Henry E. Bass, and Lee N. Bolen, "Tube method of sound-absorption measurement extended to frequencies far above cutoff," J. Acoust. Soc. Am. 62, 346-353 (1977).
- 9 K. Attenborough, "On the Acoustic Slow Wave in air-filled granular media," J. Acoust. Soc. Am. 81, 93-102 (1987).
- 10 J. C. Shipps, "Analysis of Design parameters for improved ultrasonic solid dielectric microphones," Master Thesis, University of Mississippi, (1987).